Original Research

Microbial electrosynthesis of acetate from CO_2 under hypersaline conditions

Xiaoting Zhang [a, b], Tyler Arbour [b], Daijun Zhang [c], Shiqiang Wei [a], Korneel Rabaey [b, d, *]

[a] College of Resources and Environment, Southwest University, Chongqing, 400715, China
[b] Center for Microbial Ecology and Technology (CMET), Ghent University, Coupure Links 653, 9000, Ghent, Belgium
[c] State Key Laboratory of Coal Mine Disaster Dynamics and Control, Chongqing University, Chongqing, 400044, China
[d] Center for Advanced Process Technology for Urban Resource Recovery (CAPTURE), Frieda Saeysstraat 1, 9052, Ghent, Belgium

A B S T R A C T

Microbial electrosynthesis (MES) enables the bioproduction of multicarbon compounds from CO_2 using electricity as the driver. Although high salinity can improve the energetic performance of bio-electrochemical systems, acetogenic processes under elevated salinity are poorly known. Here MES under $35-60$ g L^{-1} salinity was evaluated. Acetate production in two-chamber MES systems at 35 g L^{-1} salinity (seawater composition) gradually decreased within 60 days, both under -1.2 V cathode potential (vs. Ag/AgCl) and -1.56 A m^{-2} reductive current. Carbonate precipitation on cathodes (mostly $CaCO_3$) likely declined the production through inhibiting CO_2 supply, the direct electrode contact for acetogens and H_2 production. Upon decreasing Ca^{2+} and Mg^{2+} levels in three-chamber reactors, acetate was stably produced over 137 days along with a low cathode apparent resistance at 1.9 ± 0.6 mΩ m^2 and an average production rate at 3.80 ± 0.21 g m^{-2} d^{-1}. Increasing the salinity step-wise from 35 to 60 g L^{-1} gave the most efficient acetate production at 40 g L^{-1} salinity with average rates of acetate production and CO_2 consumption at 4.56 ± 3.09 and 7.02 ± 4.75 g m^{-2} d^{-1}, respectively. The instantaneous coulombic efficiency for VFA averaged $55.1 \pm 31.4\%$. Acetate production dropped at higher salinity likely due to the inhibited CO_2 dissolution and acetogenic metabolism. *Acetobacterium* up to 78% was enriched on cathodes as the main acetogen at 35 g L^{-1}. Under high-salinity selection, 96.5% *Acetobacterium* dominated on the cathode along with 34.0% *Sphaerochaeta* in catholyte. This research provides a first proof of concept that MES starting from CO_2 reduction can be achieved at elevated salinity.

1. Introduction

CO_2 can be converted into commodity chemicals and fuels by carbon capture and utilization (CCU) while also contributing to the reduction in atmospheric CO_2 level and providing an alternative to petroleum products [1]. Microbial electrosynthesis (MES) is a CCU route whereby microorganisms directly or indirectly use electrical current to produce organics such as acetate from CO_2 [2−5]. This process could potentially contribute to achieving a sustainable society by storing renewable energy as covalent chemical bonds based on reducing CO_2 [5,6]. MES using whole microorganisms as biocatalysts capable of self-generation and producing long-chain

organic chemicals also shows the advantages of lower over-potential, longer operational stability, and milder operational conditions [9,10], compared with systems employing abiotic CO_2 reduction catalysts [5,7,8]. Acetate is the most common bioproduct generated by MES, and although low in value and difficult to separate from water, this compound can serve as a precursor for the synthesis of many multi-carbon volatile fatty acid (VFA) compounds of higher economic value, such as caproate, via chain elongation [9]. Even so, the acetate production rate and the energy conversion efficiency obtainable from MES remain too low for economically viable application [4,10].

Acetogens remain the key microorganisms for MES using different pathways for CO_2 reduction, such as the Wood-Ljungdahl pathway [11,12]. These species have been reported to use cathodes either directly (via electron uptake) [3] or indirectly (via H_2 evolution) to reduce CO_2 into organics [10,13]. But the latter method is

* Corresponding author. Center for Microbial Ecology and Technology - FBE - Ghent University, Belgium.
E-mail address: Korneel.Rabaey@UGent.be (K. Rabaey).

increasingly applied due to higher potential rates at present [4,14]. The low acetate production rate from MES is thus associated with the low current density reached in the bioelectrochemical system (BES) for H_2 production. This density can be up to approximately 20 mA cm^{-2} but generally far below. A main reason for the low current is the high ohmic resistance resulting from the low ionic conductivity of microbial-compatible electrolytes and suboptimal spacing of electrodes or the non-ideal geometry between the membrane and microorganisms [4,15]. It appears therefore impossible yet to combine relevantly high current densities (i.e., high production rates) and relevantly low cell voltage (i.e., acceptable energy conversion efficiencies) [4]. Reducing the high ohmic resistance in BESs is therefore crucial to improve MES performance, especially for systems with high current densities or scaled-up structures due to the development trend for MES [4,6,8]. A possible solution is to use high-salinity electrolytes, as these reduce the ohmic resistance and thereby the applied voltage needed to drive a certain current density or can increase the current produced under a certain voltage [16], which would help to improve energy conversion efficiency or production rates in MES. Although some acetogens with high salinity tolerance have been reported [17,18], the knowledge in the context of MES under saline conditions is very limited.

A previous study assessed the use of brine pool sediment as inoculum and a seawater-brine interface solution as the electrolyte in MES systems to enrich halophilic homoacetogens at a biocathode operating at −1.0 V vs. Ag/AgCl. However, this system showed a limited capacity for VFA production at salinity levels of 25% and 10% along with a gradual decrease in reduction current [19]. Metal precipitates on the cathode were observed, but the impact of this precipitation on VFA production in the saline MES has not been revealed [19]. Slightly higher titer was subsequently observed at a salinity level of 3.5% using the former cathode as the inoculum. Genus *Marinobacter* and phylum Firmicutes were found to be dominant at all salinity levels examined, but no obvious acetogen was observed. *Marinobacter* was assumed to consume fixed carbon in this system, thus relating to the low VFA production [19]. Another study further examined MES performance at the salinity of 3.5% using salt marshes and mangrove sediments as inocula together with synthetic red seawater as catholyte at the same cathode potential [20]. This prior work used a porous ceramic hollow tube wrapped with carbon cloth as the cathode with a large projected area of 110 cm^2 for direct CO_2 delivery and minimizing CO_2 mass transfer limitation. A higher titer was subsequently obtained, but the production rates remained low at 1.69 g m^{-2} d^{-1} for acetic acid and 0.55 g m^{-2} d^{-1} for methane after a 10-day batch operation, while the reduction current also decreased over time [20]. During these trials, *Acetobacterium* belonging to the phylum Firmicutes exhibited unstable enrichment, which was likely related to the low acetate production rate [20]. Cathodes in the aforementioned studies were both poised at −1.0 V vs. Ag/AgCl. Notably, due to cathodic hydrogen production, the pH in the vicinity of the cathode will increase and this could lead to scale formation by the Ca^{2+} and Mg^{2+} ubiquitous in seawater and other saline streams. How this will impact the electrochemical activity and hydrogen production performance under that potential is as yet not studied, and it makes unclear whether high salinity will actually improve MES. Although the microbial community regarding CO_2 reduction in cathodic chambers under high salinity has been analyzed in previous studies [19,20], the community effectively contributing to acetate production under high salinity is also as yet not defined.

The present work investigated acetate production under saline conditions while assessing the impact and mechanism of scaling on MES. Reactors were operated stably for 137 days at the salinity of 35 g L^{-1} (seawater salinity), after which the salinity was increased to 60 g L^{-1} to study the MES performance under the elevated salinity. The microbial community composition and its contribution to acetate production in the saline MES system were analyzed based on the 16S rRNA gene and quantitative polymerase chain reaction (qPCR) analyses.

2. Materials and methods

2.1. MES setup and synthetic saline seawater

Two-chambered MES reactors were used to study the impact of Ca^{2+} and Mg^{2+} ions on VFA production at 35 g L^{-1} (seawater salinity), comprising the small (S-MES), and big MES systems (B-MES) with different sizes. An overview and a concise description of the system were shown in Fig. S1. The anode and cathode chambers were separated by a cation exchange membrane (CEM). The cathodes were carbon felt with projected surface areas of 25 and 64 cm^2 in those two systems. The total volumes of the catholyte and anolyte in both systems were 250 and 700 mL, respectively. The electrolyte was circulated using a pump at a rate of 10.5 mL min^{-1}. A second set of three-chambered big MES reactors was used to study the impact of salinity on VFA production while avoiding anodic chlorine evolution and the influence of scaling ions. This apparatus was the same as B-MES reactor except for adding an extra middle chamber of 128 mL between the anodic and cathodic chambers and an additional CEM used to separate the three chambers. The salinity was constant at 35 g L^{-1} in one of the three-chambered MES systems (3C-B$_c$-MES), but was step-wise increased from 35 to 60 g L^{-1} in the other (3C−B$_i$-MES). The volumes of catholyte and middle-chamber electrolyte were all 400 mL (Fig. S1). The operating conditions applied in different MES systems were summarized in Table 1.

A saline homoacetogen medium was used as catholyte based on the ionic composition of Atlantic seawater [21] and the media used in previous MES research [22]. The saline catholyte with 35 g L^{-1} salinity contained the following components (L^{-1}): 25.00 g NaCl, 2.50 g NaHCO$_3$, 11.00 g MgCl$_2$·6H$_2$O, 1.55 g CaCl$_2$·2H$_2$O, 0.50 g KCl, 0.25 g NH$_4$Cl, 0.20 g KH$_2$PO$_4$, 0.89 g NaBr, 2.5 mL mineral mixture [22], 2.5 mL vitamin mixture [22], and 1.0 mL tungstate-selenium solution [3]. The catholyte pH was 7.6 ± 0.2. This catholyte was used in the first three cycles of S- and B-MES systems for studying the impact of Ca^{2+} and Mg^{2+} on VFA production. In the case of 3C-B$_c$- and 3C−B$_i$-MES systems, as well as the fourth cycle of B-MES system, the catholyte had a lower hardness with concentrations of MgCl$_2$·6H$_2$O and CaCl$_2$·2H$_2$O decreasing to 1.28 and 0.20 g L^{-1}, respectively. The attendant decrease in total salinity was compensated by adding NaCl. The catholyte used in 3C−B$_i$-MES system had salinity levels of 35, 40, 45, 50, or 60 g L^{-1} based on NaCl concentrations of 30.57, 35.57, 40.57, 45.57, or 55.57 g L^{-1}, respectively. The anolyte used in S- and B-MES systems was originally made of a 0.26 M phosphate buffer with pH 7.0, but was changed to a 35 g L^{-1} Na$_2$SO$_4$ solution with pH 2.5 in 3C-B$_c$-MES system. In case of 3C−B$_i$-MES system, the Na$_2$SO$_4$ solution was also used as anolyte but with the concentrations of 35, 40, 45, 50, or 60 g L^{-1} to make the salinity level equal to its catholyte. The catholyte pH was maintained at approximately 8.5 by using a pH controller.

2.2. Inoculum and operation

An enrichment of saline homoacetogens from Atlantic North Sea sediments was used as the inoculum for S-MES with an optical density (OD$_{600}$) of 0.215 and an inoculation volume at 10% v/v of the catholyte. The inoculum was acclimated before being added to the MES using the method described in Section S-1 of the Supplementary Materials. The same volume ratio of cathodic effluent from

Table 1
The operating conditions employed for different MES systems.

MES systems	Cycles involved	Hardness in catholyte	Ca^{2+} and Mg^{2+} in catholyte (g L^{-1})	Catholyte salinity (g L^{-1})	Cathode conditions
S-MES	1st–3rd	High	Ca^{2+}: 0.42, Mg^{2+}: 1.30	35.0	−1.2 V
B-MES	1st–3rd	High	Ca^{2+}: 0.42, Mg^{2+}: 1.30	35.0	−10 mA
B-MES	4th	Low	Ca^{2+}: 0.05, Mg^{2+}: 0.15	35.0	−10 mA
3C-B_c-MES	1st[a]	High	Ca^{2+}: 0.42, Mg^{2+}: 1.30	35.0	−10 mA
3C-B_c-MES	1st–3rd	Low	Ca^{2+}: 0.05, Mg^{2+}: 0.15	35.0	−10 mA
3C−B_i-MES	1st	Low	Ca^{2+}: 0.05, Mg^{2+}: 0.15	35.0, 40.0, 45.0	−10 mA
3C−B_i-MES	2nd	Low	Ca^{2+}: 0.05, Mg^{2+}: 0.15	45.0, 50.0, 60.0	−10 mA

[a] Without inoculation.

the MES system producing acetate was also used as the inoculum for the subsequent reactor (e.g., using catholyte of S-MES as the inoculum for B-MES). The reactors were built in the order of S-MES, B-MES, 3C-B_c-MES, and 3C-B_i-MES.

S-MES system was operated with the cathode poised at −1.2 V vs. Ag/AgCl, while B-MES, 3C-B_c-MES, and 3C−B_i-MES systems were operated under galvanostatic control with a constant reductive current of −10 mA (equal to a current density of −1.56 A m^{-2}; see Section S-1). To maintain anaerobic conditions in these reactors, the cathode chambers were also continuously purged by the mixed gas of N_2:CO_2 (90:10) with a flow rate of 29.7 ± 7.8 L d^{-1} using gas flow meters (OMA-1, Dwyer, UK) [21]. This gas also served as a buffering agent and a constant source of CO_2 besides sodium bicarbonate in catholyte. The effluent gas from the cathodic chamber flowed through the anodic chamber to strip O_2 produced at the anode. These experiments were conducted in the batch mode at ambient temperature, and the cycle's start and end time were depended on the change of acetate production during the cycle (see Section S-1). At the end of each cycle, all catholyte in S-MES system was refreshed, but only 90% of the catholyte in B-MES, 3C-B_c-MES, and 3C−B_i-MES systems was replaced. The remaining 10% was kept in the reactor acting an inoculum for subsequent operations. The salinity in 3C−B_i-MES system was increased by adding NaCl to the catholyte supernatant. This supernatant was obtained by centrifuging the catholyte at 6000 rpm for 20 min to separate the biomass. Following this, the separated biomass and the dissolved NaCl were added back into the cathodic chamber to reduce any effects on the existing microbial community.

2.3. Calculations and analyses

During the experiments, liquid samples were taken and filtered (0.22 μm cut-off) for monitoring VFAs, Cl^-, Ca^{2+}, and Mg^{2+} concentrations by ion chromatography (IC). Unfiltered samples were used for determining pH. The effluent gases from each reactor were analyzed using a compact gas chromatograph (GC). Surface elements of the used and clean cathodes were analyzed by scanning electron microscopy (SEM) coupled with an energy dispersive X-ray spectroscopy (EDX) detector. Precipitate compositions were analyzed using X-ray diffractometer (XRD). The details of these analyses were provided in Section S-1.

Cyclic voltammograms (CVs) of the cathodes were conducted with a scan rate of 1 mV s^{-1} under constant N_2:CO_2 purging conditions. The initial scan range was from 0.2 to −1.0 V (all values vs. Ag/AgCl) but was adjusted to −0.4 to −1.4 V based on the change of cathode potentials in different reactors. The current density was calculated as the amount of electric current flowing per projected cathode surface area [6]. The coulombic efficiency (CE, %) of the cathodes for cumulative VFA and H_2 production and the CO_2 consumption rate, R_{CO_2}, were calculated based on prior work [20,22−24], shown as follows.

$$CE_{VFA} = \frac{n_{v,t} \times f_{e,v} \times F}{\int_{t=0}^{t} I dt} \times 100 \tag{1}$$

$$CE_{H_2} = \frac{n_{H_2} \times 2F}{\int_{t=0}^{t} I dt} \times 100 \tag{2}$$

$$R_{CO_2} = 1.05 \times \text{acetate production rate } \left(\text{in g m}^{-2} \text{ d}^{-1}\right) \times 2 \div 60 \times 44 \tag{3}$$

Here, $n_{v,t}$ and n_{H_2} are the moles of the VFAs and H_2 produced at time t, $f_{e,v}$ is the molar conversion factor of produced VFA (it is 2 for formate, 8 for acetate, 14 for propionate, and 20 for butyrate and isobutyrate), I is the current (A), and F is Faraday's constant (96,485 C mol^{-1}). The acetate production rate and the instantaneous CE were calculated based on the different VFA concentrations between two consecutive measurement points within one cycle (see Section S-1).

2.4. Microbial community composition

After the trials using the B-MES, 3C-B_c-MES, and 3C−B_i-MES systems were complete, the cathodes were removed for microbial community analysis (named as B−C, 3C-B_c-C, and 3C−B_i−C). Catholyte samples of 35 g L^{-1} salinity that acquired at the end of B-MES system trials (B−P) and at the end of the first, second and third cycles of 3C-B_c-MES system (the 3C-B_c-P-1, 3C-B_c-P-2, and 3C-B_c-P-3 samples) were also subjected to microbial community analysis. In addition, catholyte from 3C−B_i-MES system with salinity levels of 45, 50, and 60 g L^{-1} (3C−B_i−P-45g, 3C−B_i−P-50g, and 3C−B_i−P-60g samples) were also assessed. The microbial community was determined using V3−V4 region of the 16S rRNA gene, while the absolute abundances of bacteria from the cathode and catholyte of 3C−B_i-MES system were estimated by qPCR. The details of the DNA extraction, V3−V4 region amplification, Illumina 16S rRNA gene amplicon construction and qPCR of 16S rDNA are provided in Section S-1 of the Supplementary Materials. The raw sequencing data of those samples has been deposited in NCBI Sequence Read Archive (accession No. SRP395816).

3. Results and discussion

3.1. Unstable acetate production under a potentiostatic condition

Acetate was produced in S-MES system with a cathode potential of −1.2 V using simulated seawater as catholyte but not unstably (Fig. 1), which also occurred in previous studies [20,25]. Acetate along with small amounts of formate and propionate was produced in this system during three successive cycles. However, the peak
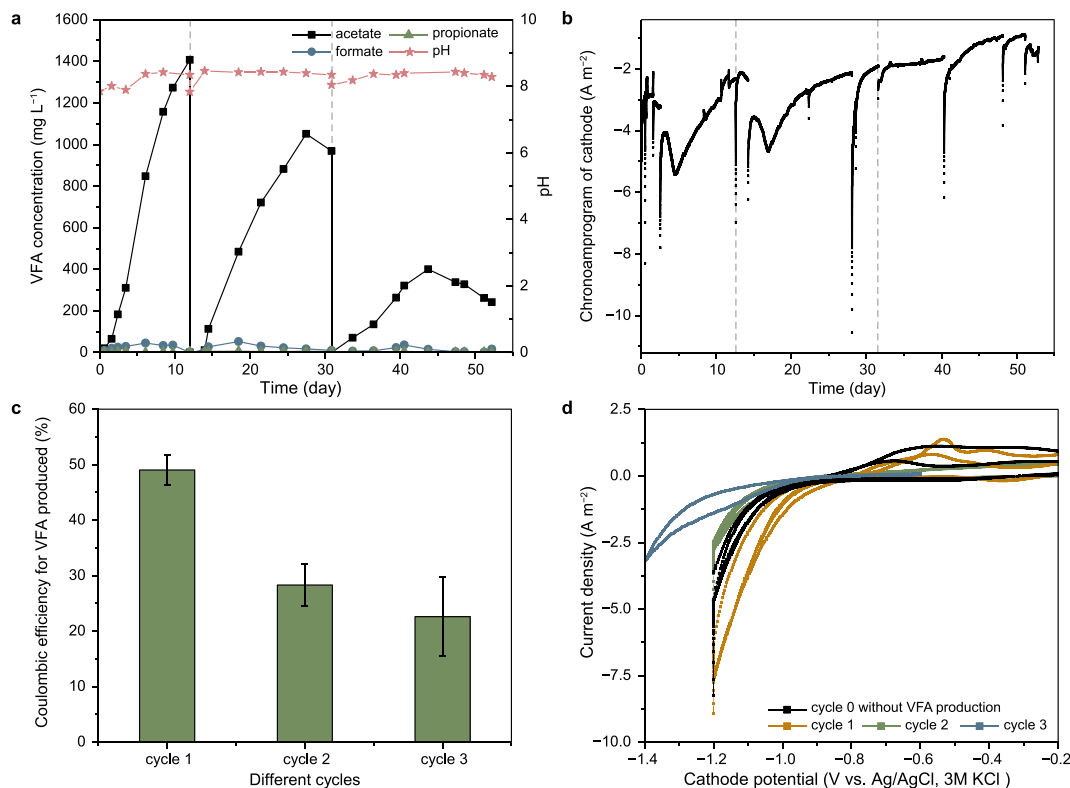
Fig. 1. Acetate production performance of S-MES with cathode poised at −1.2 V vs Ag/AgCl using simulated seawater as catholyte. **a**, VFA production; **b**, The chronoamperogram of the cathode; **c**, Coulombic efficiency for cumulative VFA production; **d**, Cathode CV scan results.

acetate concentration gradually decreased for each cycle, reaching 1,407, 969, and 400 mg L^{-1}, respectively (Fig. 1a). The maximum production rate (R_{max}) also decreased from 20.15 to 9.27 then to 5.44 g m^{-2} d^{-1}, accompanied by a decline in the average acetate production rate (R_{avg}) from 9.28 ± 6.34 to 3.85 ± 4.09 then to 0.99 ± 2.78 g m^{-2} d^{-1} (Fig. S2). A decrease in the reductive current at −1.2 V was observed during these cycles (Fig. 1b). The CE for cumulative VFAs in each cycle also decreased, from 49.1 ± 0.1% to 22.6 ± 0.1% (Fig. 1c and Fig. S2c), suggesting that the energy conversion efficiency was lowered. In addition, although H_2 was detected prior to inoculation, the gradual decrease in the reductive current and the relatively high purge rate resulted in a minimal amount of residual H_2 at the end of each cycle after consumption by microbes. But the electron involved in residual H_2 may also contribute to the low CE. The decrease in the reductive current density was also confirmed by CV characterization (with −7.66, −7.0, and −1.43 A m^{-2} at −1.2 V in cycle 1, 2, and 3, respectively, Fig. 1d). The CV results indicated an increasingly weak electrochemical activity of the cathode for H_2 production.

A white coating was observed forming on the S-MES system cathode during these experiments. The SEM-EDX analysis revealed that those precipitates mostly contained Ca with minor amounts of Mg and P (Fig. 2). The XRD analysis further indicated that the white precipitates primarily comprised $CaCO_3$ (JCPDS No. 84−0049) (Fig. 2c). These results agreed with the production of numerous bubbles during the dissolution of these precipitates with 1.00 M HCl (Fig. S3) and the higher mass-based ratio of Ca^{2+} to Mg^{2+} in the resulting solution (1.50) compared with the original simulated seawater (0.32). NaCl was also found in this precipitate due to the use of saline catholyte (JCPDS No. 78−0751). Those insulating carbonate precipitates likely hindered the direct contact between both water (acting as a hydroxyl ions source) and microbes with the

cathode surface and thus inhibited H_2 production. The direct contact between the cathode and acetogens may be also important for acetate production, because microbes have been reported to add catalysts at the cathode surface to facilitate CO_2 reduction by producing intermediates [15].

3.2. Unstable acetate production at a −10 mA reductive current

To eliminate the impact of insufficient H_2 generation on acetate production, the acetate production using simulated seawater as catholyte was further studied at a reductive current density of −1.56 A m^{-2} in B-MES system with a constant H_2 yield. In this trial, acetate was again the main product, along with minor amounts of propionate and butyrate (Fig. 3a). Formate was also detected during the first two cycles, likely because of the high catholyte pH (8.43−8.85) during the second half of cycle 1 (Fig. 3a) [13]. It should be noted that the acetate production was again unstable and the peak acetate concentration decreased from 1287 mg L^{-1} in cycle 1 to 783 mg L^{-1} in cycle 3 (Fig. 3a). The R_{max} also decreased from 8.52 in cycle 1 to 3.06 g m^{-2} d^{-1} in cycle 3 (Figs. S4a−c) and R_{avg} declined from 2.99 ± 2.73 to −0.30 ± 3.92 g m^{-2} d^{-1}. The average CE for cumulative VFA production stabilized at 19.2 ± 1.5% in cycle 1 but sharply decreased to 4.5% in cycle 3 (Fig. S4g) along with a gradual increase in the system voltage from 2.58 to approximately 2.66 V (Fig. S4e). The CEs for H_2 at the end of these cycles were within 16.0−22.0%. A higher instantaneous CE for VFA production was observed in conjunction with a high acetate production rate during cycle 1, such as 61.5% on day 19 and 86.0% on day 23 (Fig. S4g). These data indicated that the low amount of microbes at the beginning of cycle 1 may contribute to the low CE for VFA generation. But this CE remained low during cycles 2 and 3 and even became negative during the second half of cycle 3 (Fig. S4h), which suggested that the
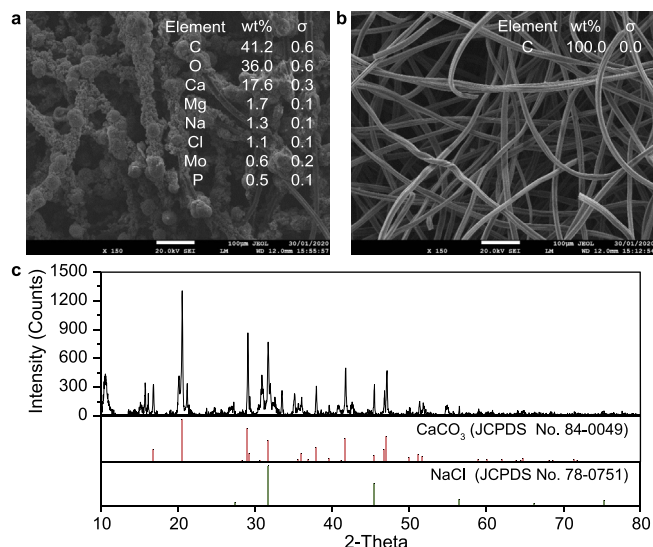
Fig. 2. **a**−**b**, SEM-EDX micrographs of the S-MES cathode after the experiment with precipitation on the electrode surface (**a**) and a new cathode before the experiment (**b**). **c**, The XRD patterns of the white precipitate and pure $CaCO_3$ and NaCl.

reduction of CO_2 to generate VFAs was inhibited, and a portion of VFAs was likely converted to other compounds or consumed by microbes [19]. The pH at the end of each cycle stabilized at approximately 8.5, and white precipitates were again deposited on the cathode surface (Fig. S3c). Because the H_2 yield was constant due to the constant reductive current, the carbonate precipitates could possibly reduce both the CO_2 supply and H_2 utilization, leading to a decrease in CE related to VFA production.

To address the scaling issue, the hardness of the catholyte used in cycle 4 was lowered as described in Section 2.1, following which stable acetate production was achieved. The catholyte pH remained at approximately 8.5, but the acetate concentration continually increased over the remaining 60 days, reaching a value of 5193 mg L^{-1} (Fig. 3a) along with a R_{avg} of 3.51 ± 1.69 gm^{-2} d^{-1}. The average CE for cumulative VFA production also increased to 25.1 ± 4.4%, and the instantaneous CE at the end of the cycle was significantly higher at 58.3%, along with a low CE for residual H_2 of 5.3% (Fig. S4g). These results were consistent with the observed decrease in cell voltage to 2.55 V (Fig. S4e) and the recovery in the cathode potential from −1.42 to −1.34 V (Fig. S4f). Successive CV data showed obviously higher reductive current at −1.34 V indicating a more rapid H_2 removal from the cathode surface by

microbes (Fig. 3b) [22]. The alkaline pH in the vicinity of the cathode resulting from cathodic hydrogen production likely favored carbonate formation and thus generated primarily $CaCO_3$. Therefore, the carbonate precipitates further decreased CO_2 availability and also inhibited H_2 generation and its utilization by acetogens. The formation of calcium carbonate precipitates was likely the main reason for the unstable acetate production in these MES systems under saline conditions.

3.3. Stable long-term acetate production at −10 mA in a three-chambered BES

The 3C-B_c-MES system was constructed to further investigate stable acetate production under saline conditions while avoiding the common phenomenon of chloride oxidation at the anode [20]. In this system, the anolyte was a low-pH Na_2SO_4 solution to enhance the proton supply to catholyte. But in the trail using synthetic seawater as catholyte and the Na_2SO_4 solution as anolyte in this system without inoculation, tight white precipitates were again formed on the cathode surface and obviously inhibited the cathode electrochemical activity (Fig. S5). Thus, the catholyte was replaced with synthetic seawater with a lower hardness, as described in Section 2.1.

Stable acetate production was obtained using this system during three batch cycles throughout 137 days (Fig. 4). The cumulative acetate concentration was as high as 3440 mg L^{-1} within a single cycle, and the R_{max} reached 8.99 ± 1.30 g m^{-2} d^{-1} along with a R_{avg} of 3.80 ± 0.21 g m^{-2} d^{-1} during these three cycles. One mole of acetate production is equivalent to 2 mol of CO_2 fixation, and the biomass of chemolithoautotrophic microbes producing acetate from CO_2 and H_2 was reported to accounted for 5% of the carbon flux [23,24]. Therefore, the maximum CO_2 consumption rate was 13.84 ± 2.01 g m^{-2} d^{-1} and the average was 5.94 ± 0.30 g m^{-2} d^{-1}. The average CE for cumulative VFA production during these three cycles was 36.0 ± 3.0% (Fig. 4c), essentially entirely as acetate (34.4 ± 3.2%). The instantaneous CE for VFA generation was also higher during the second half of each cycle, with average values of 42.2 ± 19.8%, 45.7 ± 23.3%, and 40.1 ± 16.9% for cycles 1, 2, and 3, respectively (Fig. S6). These data also suggested limited usage of H_2 by low amounts of microbes at the beginning of the cycle, leading to the relatively low CE for cumulative VFA. The instantaneous CE for H_2 during these cycles fluctuated within the range of 11.3−34.0%, likely due to the relatively high flow rate of the mixed gas. Methane formation was not detected, but some electrons may also have ended up in the biomass. The CV results shown in Fig. 4d confirmed that this cathode exhibited more stable and higher electrochemical
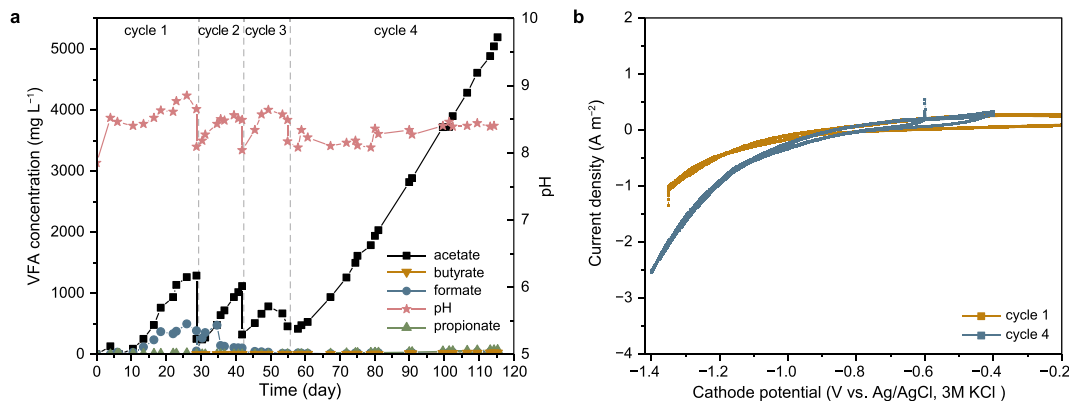

Fig. 3. Acetate production performance of B-MES with a reductive current density of −1.56 A m^{-2} using simulated seawater as catholyte during the first three cycles but lower Ca^{2+} and Mg^{2+} concentrations in cycle 4. **a**, VFA production; **b**, Cathode CV scan results.

activity during long-term operation likely due to the absence of precipitation on the cathode surface when compared with the B-MES system. An oxidative peak at approximately -0.57 V (vs. Ag/AgCl) was observed, but probably did not play an important role as the actual cathode potential was much lower [22]. A stable, lower voltage of approximately 2.45 V was obtained (Fig. 4b) along with a higher cathode potential of approximately -1.23 V. These results could be attributed to the low energy losses in this system without the formation of precipitates on the cathode.

Because these systems were purged solely with 10% CO_2 at a relatively high rate and operated at a low current density, the VFA production rate was likely slowed. Even so, this rate was still much higher than those observed in prior studies using the same salinity (0.95 and 0.46 g m^{-2} d^{-1} for acetate and formate, respectively [19], and 1.69 and 0.55 g m^{-2} d^{-1} for acetic acid and methane, all based on projected cathode area, respectively) [20]. The apparent resistance of cathode, as determined by the current interrupt method [26] showed a quite low level of 1.9 ± 0.6 mΩ m^2 for the present system (Fig. S7) and thus agreed with the high catholyte conductivity of 50.1 ± 0.8 mS cm^{-1} at the end of the cycle (Fig. S8). This resistance was much higher in B-MES and S-MES systems with 71.8 and 6.4 mΩ m^2, respectively, likely due to precipitation on their cathode surfaces. BESs have been reported to show higher area-specific ohmic resistance, typically higher than 10 mΩ m^2 because of the low ionic conductivity of microbial compatible catholyte (generally around 10 mS cm^{-1}) [4,26]. Considering that the electrolysis of water typically proceeds at the anode, this low apparent resistance of cathode would be expected to greatly affect the energy efficiency of MES, especially at high current densities [4,8]. The voltage used in this research was lower than values used in prior studies but was combined with a higher current density (Table S1), further confirming the decreased energy input required by highly saline MES processes. In addition, because the CEM was permeable to salt [27], chloride appeared in the anolyte of this system. But significantly more chloride was accumulated in the middle chamber and thus subsequently prevented severe chloride oxidation on the anode (Fig. S9).

3.4. Acetate production with elevated salinity at -10 mA

Building on the stable performance of MES in 3C-B$_c$-MES system, another three-chamber MES system (designated 3C$-$B$_i$-MES) was constructed to investigate acetate production at increasingly elevated salinity levels between 35 and 60 g L^{-1}. The catholyte conductivity at each salinity gradually increased from 48.7 to 78.1 mS cm^{-1} (Fig. S8), which was consistent with the salinity settings. Acetate was continually produced when the salinity was gradually increased from 35 to 50 g L^{-1}, resulting in significant accumulation of this product (Fig. 5a). However, R_{max} gradually decreased to 8.94, 8.70, 5.47, and 4.21 g m^{-2} d^{-1} at salinity levels of 35, 40, 45, and 50 g L^{-1}, respectively, while R_{avg} stabilized at 3.93 ± 2.01, 4.56 ± 3.09, 3.24 ± 1.51, and 3.31 ± 0.71 g m^{-2} d^{-1} under each salinity (Fig. S10). The maximum CO_2 consumption rates at these same salinity levels were 13.77, 13.40, 8.42, and 6.48 g m^{-2} d^{-1}, respectively, while the average values were 6.05 ± 3.10, 7.02 ± 4.75, 4.50 ± 2.32, and 5.10 ± 1.10 g m^{-2} d^{-1}, respectivley [23,24]. The average CEs for cumulative VFA production were $32.2 \pm 3.0\%$, $38.6 \pm 3.3\%$, $35.6 \pm 5.4\%$, and $30.4 \pm 1.1\%$, respectively, at each salinity (Fig. 5c). The instantaneous CEs for VFA production were again higher than the CE for cumulative VFA production, especially at salinity levels of 35 and 40 g L^{-1} with average values of $43.4 \pm 22.5\%$ and $55.1 \pm 31.4\%$, respectively (Fig. S10d), which also suggested limited uptake of H_2 by the low amounts of microbes at the beginning of the cycle. The instantaneous CE for VFA production at 45 and 50 g L^{-1} were substantially

reduced to $24.7 \pm 16.0\%$ and $32.4 \pm 7.5\%$, respectively, along with the decreases in the instantaneous CEs for H_2 generation at the end of the operating period from 5.3% at 35 g L^{-1} to 2.6% at 50 g L^{-1}. These results indicated the inhibition of CO_2 reduction to VFAs at higher salinity. When the salinity was further increased to 60 g L^{-1}, acetate production was inhibited in the first eight days and then recovered in the following days, but the average production rate and CE were very low (Fig. 5c and Fig. S10d) which could possibly be attributed to adaption of the acetogens.

Notably, the system voltage also gradually declined from 2.45 to 2.29 V (Fig. 5b), while the cathode potential gradually rose from -1.19 to -1.07 V (Fig. S10e) upon raising the salinity from 35 to 40 g L^{-1} and remained at this level as the salinity increased above 40 g L^{-1}. The apparent resistance of cathode also gradually decreased from 1.9 mΩ m^2 at 35 g L^{-1} to 1.2 mΩ m^2 at 60 g L^{-1} (Fig. S7). The slight decrease in the system voltage could be attributed to the very low apparent resistance at these salinity levels. The CV data demonstrated that the cathode activity was significantly improved as the salinity was increased (Fig. 5d). Specially, H_2 evolution potential was -0.97 V at 35 g L^{-1} after inoculation but increased to -0.90 V at salinity levles within the range of $45-60$ g L^{-1} (Fig. 5d). The extent to which CO_2 dissolves has been reported to decrease at high salinity, which would, in turn, be expected to lower the production of VFAs [19,20,28]. Thus, the highest CE appeared at 40 g L^{-1} likely due to the decreased cell voltage and a presumably slight decrease in CO_2 solubility at this salinity. The inhibited VFA production at higher salinity may also relate to the energy conservation because microbes may produce organic compatible solutes such as ectoine due to osmotic adaption [19,29].

In addition, when the salinity was no less than 45 g L^{-1}, a redox couple appeared during CV scan with an oxidative peak at approximately -0.71 V and reductive peak at -1.08 V. The half-saturation potential (E_M) of this redox couple was -0.90 V, which was similar to the H_2 evolution potential at high salinity. However, this redox couple was unstable as these peaks became increasingly weak with continued CV scans (Fig. S11). But the peaks returned following an extended period of polarization, which was in agreement with the previous research in which an oxidative peak corresponding to H_2 oxidation was significantly enhanced after a prolonged polarization period when using a microbes-covered graphite electrode [30]. This phenomenon may be related to enzyme activation processes induced by extended electrode polarization [30]. Therefore, this couple may be associated with the shift in cathode potential and the significantly increased reductive current at high salinity. As no similar reductive peak was observed in the present MES systems at the salinity of 35 g L^{-1}, so this redox couple might represent a unique feature of the microbial communities that developed at salinity levels higher than 35 g L^{-1}, as discussed below (Section 3. 5.2).

3.5. Microbial community analysis

The SEM images of cathodes used in these systems (Fig. 6) show that biofilms were successfully formed on the cathode surfaces in the three-chambered systems of 3C-B$_c$- and 3C$-$B$_i$-MES with low-hardness catholyte. Microbes were also found on cathodes from both S- and B-MES systems but primarily on the surfaces of thick $CaCO_3$ precipitates that deposited on the cathode surfaces. Those outcomes concurred with the inhibited cathode electrochemical activity and acetate production in those two systems.

3.5.1. The effects of scaling ions on MES microbial activity

Firmicutes, Proteobacteria, Actinobacteria, and Bacteroidetes were the dominant phyla in B-MES system but with obviously higher relative abundances of the first two phyla (together
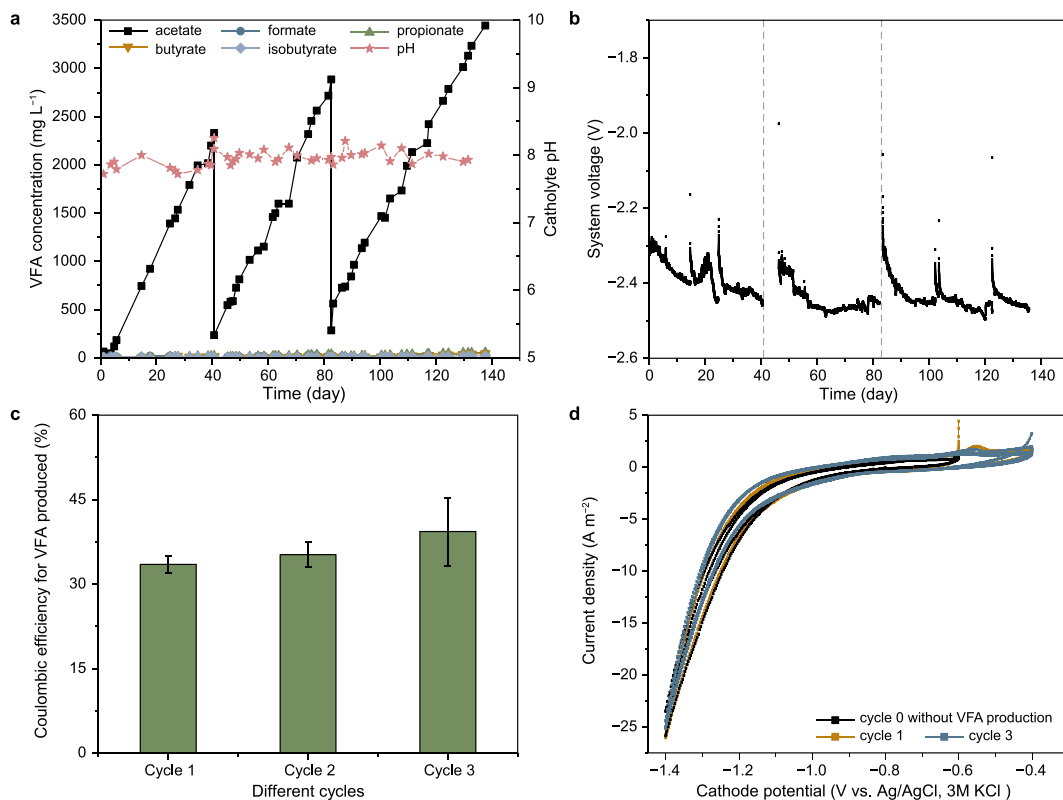
Fig. 4. Stable acetate production performance of 3C-B_c-MES at seawater salinity (35 g L^{-1}) with low Ca^{2+} and Mg^{2+} concentrations. **a**, VFA production; **b**, System voltage; **c**, Coulombic efficiency based on cumulative VFA production; **d**, Cathode CV scan results.

accounting for 85−91%). Firmicutes were highly enriched on the cathode (75.8%), but more Proteobacteria were accumulated in catholyte (58.7%) (Fig. S12). These two phyla were also accumulated in 3C-B_c-MES system with the same trends. Firmicutes, Proteobacteria, and Actinobacteria have been reported to contain many CO_2-assimilating microorganisms [11]. Additionally, minimal Epsilonbacteraeota were enriched in all catholyte, while Spirochaetes were only obviously enriched in the 3C-B_c-catholyte.

In genus level, the most abundant acetogen accumulating on the cathode in both B-MES and 3C-B_c-MES systems was the canonical homoacetogen *Acetobacterium* [31], with relative abundances of 67.1% and 78%, respectively (Fig. 7). This genus was very likely the primary carbon fixer reducing CO_2 to acetate via the Wood-Ljungdahl pathway, and probably did a significant contribution to VFA production in these systems [15]. This genus was also found in catholyte but at much lower levels (19.8% in B−P and 3.8% in 3C-B_c-P). Such results concurred with previous studies, which suggested that the cathode and biocatalyst should be in close proximity to one another to facilitate the transfer of electron mediators such as H_2 during CO_2 reduction [6,15]. Therefore, the direct contact with the cathode was evidently important for acetate formation. The carbonate precipitates likely restricted this direct contact between the acetogens and the cathode and also limited the CO_2 supply, leading to weakened cathode electrochemical activity. The proportion of *Acetobacterium* in 3C-B_c-P catholyte samples also decreased from 19.0% to 3.8% during the batch cycles. This decrease could probably be attributed to the lower Ca^{2+} and Mg^{2+} levels in catholyte that, in turn, led to better contact with the electrode. As such, the metabolism of this dominant genus on the cathode was promoted, and the H_2 concentration in the catholyte was decreased. Some other acetate-producing genera were also accumulated in these systems but with much lower proportions, within the range of 4.4−8.8%,

including Clostridiaceae_2_unclassified, Propionibacteriaceae_unclassified, and *Sphaerochaeta*.

Besides, *Pseudomonas* was the most abundant genus in catholyte with 56.7% in B−P and 68.4−71.9% in 3C-B_c-P, but with obviously lower proportions on the cathode (11.6−13.6%) (Fig. 7). This genus has been reported to be highly enriched both on the cathode and in catholyte of MES systems for industrial CO_2 reduction (up to 26% relative abundance) and was thought to promote extracellular electron transfer and hydrocarbon removal [31−33]. The exoelectrogenic genus *Arcobacter* present in the catholyte of 3C-B_c-P with 7.0% might associate with the enrichment of *Pseudomonas* producing electron mediators. The significant proportion of *Pseudomonas* in the catholyte may also affect both H_2 oxidation and acetate consumption in the system, because of its hydrogenase activity and fermentation capacity [33,34], but further study is required to definitively assess the function of this genus in such systems. Finally, the fermentative genus *Bacteroidia*_unclassified was gradually accumulated in 3C-B_c-P with relative abundance of 7.0%, 6.3%, and 11.2% at the end of cycles 1, 2, and 3, respectively. These microbes' presence and activity might help explain the low acetate production rate at the beginning of the cycle.

3.5.2. Microbes contributing to efficient VFA production at high salinity

In the 3C−B_i-MES system, only Firmicutes (96.6%) and Proteobacteria (1.5%) were accumulated on the cathode at 60 g L^{-1} salinity likely due to the high salinity tolerance and unique ability of these phyla to acquire energy on the cathode under highly saline conditions (Fig. S12). The dominant phyla in catholyte at this salinity mainly contained Proteobacteria (57.0%) and Spirochaetaceae (34.0%).

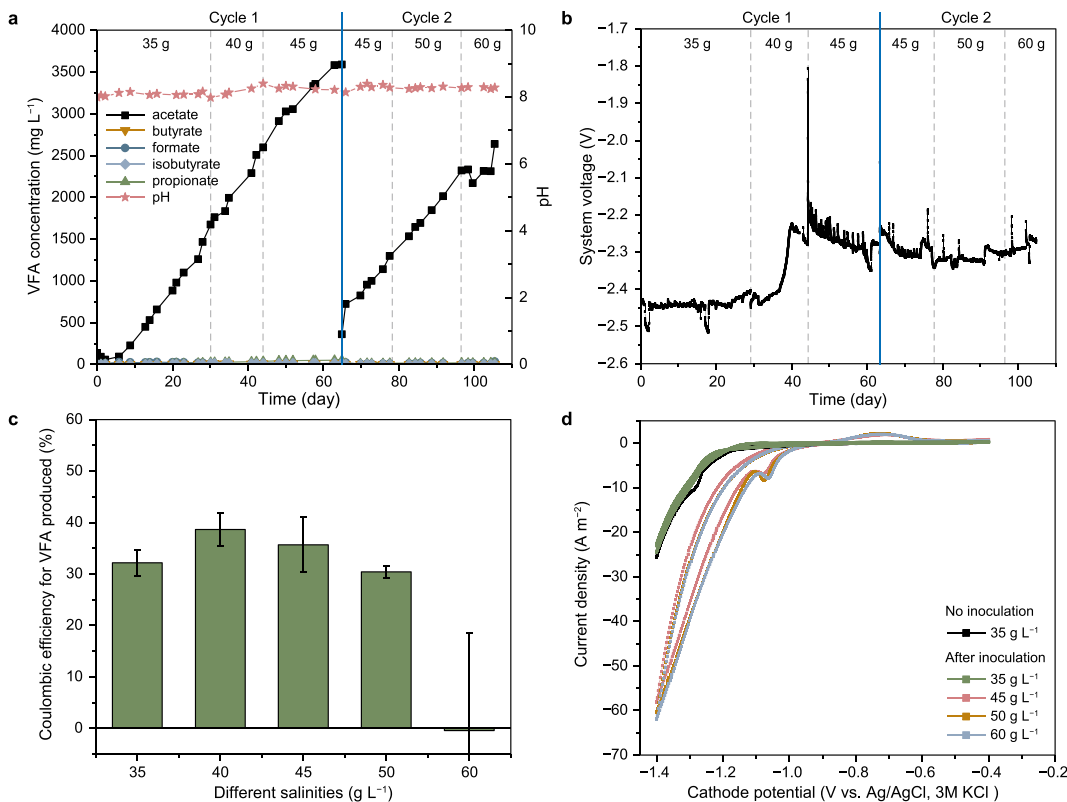*Acetobacterium* was essentially the only genus on the cathode,

Fig. 5. Acetate production performance of 3C−B$_i$-MES as the salinity gradually increased from 35 to 60 g L^{-1} in conjunction with low Ca^{2+} and Mg^{2+} concentrations. **a**, VFA production; **b**, System voltage; **c**, Coulombic efficiency for cumulative VFA production; **d**, Cathode CV scan results.

with a proportion of 96.5%. However, the proportion of this genus in catholyte was much lower, which increased from an initial value of 2.3% to 11.0% as the salinity was gradually increased to 45 g L^{-1} but then decreased to 1.1% at 50 g L^{-1} and 0.4% at 60 g L^{-1}. These results could be related to low CO$_2$ solubility [35], a reduced H$_2$ concentration in the catholyte, and a possibly inhibited metabolism of this microbe at high salinity. The proportions of the other acetate-producing genera, including *Arcobacter*, *Propionibacteriaceae*_unclassified, and *Clostridiaceae* spp., were also significantly decreased to very low levels (below 2%), likely also due to the limited tolerance of these microbes to the high salinity. These lower amounts of these genera probably also related to the decrease in acetate production under hypersaline conditions. Nevertheless, certain genera tolerable to high salinity were gradually enriched in catholyte as the salinity was increased, such as *Sphaerochaeta* which went from an initial proportion of 1.7% to 17.3% at 45 g L^{-1} and then to 33.5% and 34.0% at 50 and 60 g L^{-1}, respectively. This accumulation could be attributed to the halophilic nature of this genus and its capacity for oxidative acetogenesis under highly saline conditions [32,36]. The generation of H$_2$ and CO$_2$ by this genus may benefit the metabolisms of other acetogens in catholyte at high salinity. *Halomonas* and *Shewanella* tolerant of high salinity were both also gradually accumulated in catholyte at salinity levels of 50 and 60 g L^{-1} within 2.5−1.5%. Meanwhile, *Pseudomonas* remained the most abundant genus in catholyte, decreasing from an initial abundance of 77% to 58.6% at 45 g L^{-1}, and 48.5% and 51.3% at 50 and 60 g L^{-1}, respectively. But the proportion of this genus on the cathode was only 1.4%, suggesting low electrochemical activity at high salinity. In addition, *Bacteroides* was also accumulated only in catholyte to proportions of 1.7−4.9% with salinity increases, likely due to the low acetate production rate.

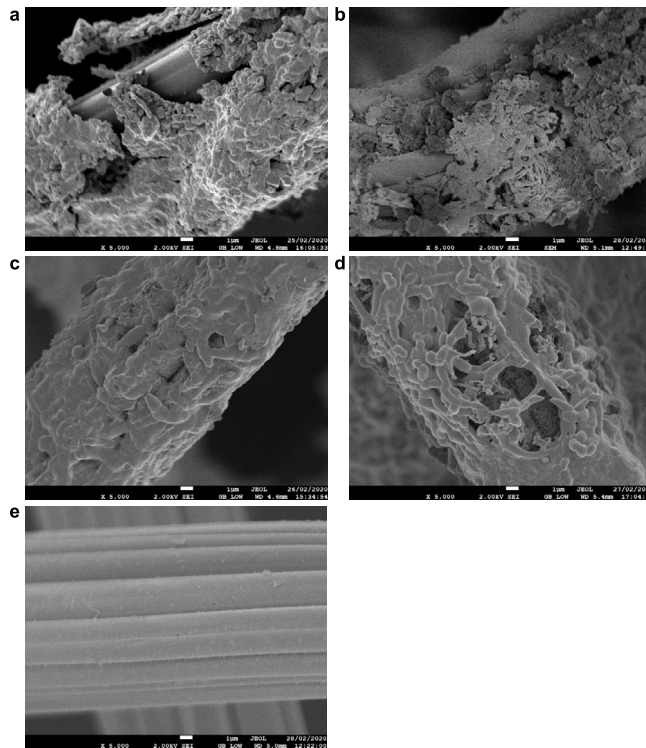According to the qPCR analysis shown in Fig. S13, the absolute

Fig. 6. SEM images of biofilms on cathodes from different systems and of the blank cathode. **a**, S-MES; **b**, B-MES; **c**, 3C-B$_c$-MES; **d**, 3C−B$_i$-MES systems; **e**, The blank cathode.
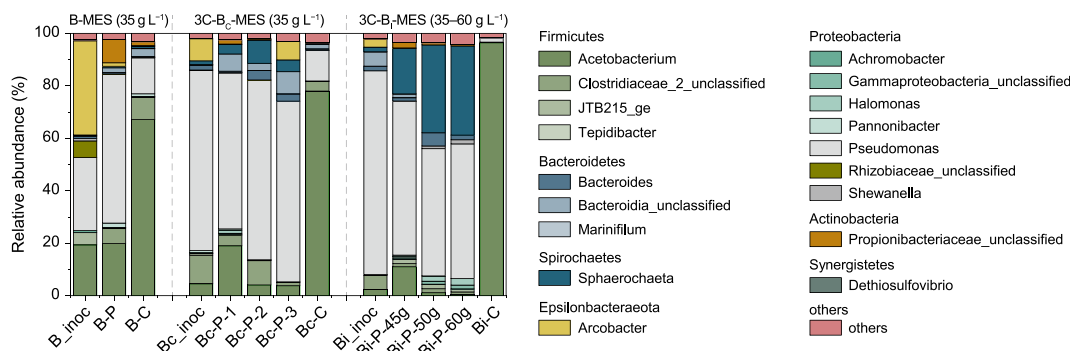
Fig. 7. Microbial community composition of the cathode and catholyte consortia from B-MES, 3C-B$_c$-MES, and 3C−B$_i$-MES systems in genus level over 1% based on 16S rRNA gene analysis.

abundance of *Acetobacterium* was 3.46×10^{11} copies on the cathode, which was 238 times higher than that in catholyte (with an initial value of 9.22×10^8 followed by an increase to 1.00×10^{10} at 45 g L^{-1} but decreases to 3.38×10^9 and 1.46×10^9 at salinity levels of 50 and 60 g L^{-1}, respectively). Furthermore, even taking all the copies of acetogens in catholyte into account, including *Arcobacter*, *Propionibacteriaceae*_unclassified, *Clostridiaceae*_2_unclassified, and *Sphaerochaeta*, the total amount was still much lower (with copies of 1.25×10^{11}, 1.18×10^{11} and 1.47×10^{11} at 45, 50, and 60 g L^{-1}). Thus, the *Acetobacterium* on the cathode likely played a significant role in VFA production within this highly saline system. But the change in the absolute abundance in catholyte provided further evidence that this genus exhibits a suitable metabolism at salinity below 45 g L^{-1} but a highly inhibited metabolism at 50 and 60 g L^{-1}. In combination with the special redox couple observed during the cathode CV scans at salinity above 40 g L^{-1}, the pronounced accumulation of this genus on the cathode might indicate a specific extracellular electron transfer pathway in *Acetobacterium* that supports its metabolism along with inhibited VFA production, but a further study is required. In addition, the special enrichment of *Sphaerochaeta* in the catholyte (with an increase from the initial copies of 6.7×10^8 to 1.58×10^{10} at 45 g L^{-1} and to 1.01×10^{11} and 1.27×10^{11} at 50 and 60 g L^{-1}, respectively) might also relate to the redox couple appearing during the CV scans at salinity levels no less than 45 g L^{-1}.

Overall, *Acetobacterium* was evidently the key acetogen for VFA production in the present MES system under hypersaline conditions and primarily accumulated on the cathode. The special accumulation of *Sphaerochaeta* in the catholyte may also contribute to acetate production. The lower acetate production rates observed at salinity levels higher than 40 g L^{-1} presumably resulted from the limited CO$_2$ solubility and the partial inhibition of acetogenic metabolism at high salinity.

4. Conclusions

Carbonate precipitating on cathodes (primarily as CaCO$_3$) was the critical reason for the unstable acetate production in MES systems fed with simulated seawater, likely through inhibiting the CO$_2$ supply, the direct electrode contact with acetogens and H$_2$ production. Stable acetate production by MES at seawater salinity was achieved along with a decreased system voltage and a very low apparent resistance of cathode, and further confirmed the potential in decreasing the energy input at high current densities by using the highly saline MES. The most efficient acetate production was obtained at the salinity of 40 g L^{-1}, because limited CO$_2$ dissolution and restrained acetogen metabolism at higher salinity probably inhibited acetate production. *Acetobacterium*,

*Clostridiaceae*_2_unclassified, *Arcobacter*, and *Spirochaetaceae* were likely the main acetogens at seawater salinity. But under high-salinity selection, 96.5% *Acetobacterium* dominating on the cathode along with 34.0% *Sphaerochaeta* in catholyte, were presumably to be the key acetogens.

Declaration of competing interest

The authors declare that they have no known competing financial interests or personal relationships that could have appeared to influence the work reported in this paper.

Appendix A. Supplementary data

Supplementary data to this article can be found online at https://doi.org/10.1016/j.ese.2022.100211.

References

[1] Z. Liu, K. Wang, Y. Chen, T. Tan, J. Nielsen, Third-generation biorefineries as the means to produce fuels and chemicals from CO$_2$, Nature Catalysis 3 (3) (2020) 274−288.

[2] L. Lu, W. Vakki, J.A. Aguiar, C. Xiao, K. Hurst, M. Fairchild, X. Chen, F. Yang, J. Gu, Z.J. Ren, Unbiased solar H2 production with current density up to 23 mA cm^{-2} by Swiss-cheese black Si coupled with wastewater bioanode, Energy Environ. Sci. 12 (3) (2019) 1088−1099.

[3] K.P. Nevin, T.L. Woodard, A.E. Franks, Z.M. Summers, D.R. Lovley, Microbial electrosynthesis: feeding microbes electricity to convert carbon dioxide and water to multicarbon extracellular organic compounds, mBio 1 (2) (2010) e00103−e00110.

[4] A. Prevoteau, J.M. Carvajal-Arroyo, R. Ganigue, K. Rabaey, Microbial electrosynthesis from CO$_2$: forever a promise? Curr. Opin. Biotechnol. 62 (2020) 48−57.

[5] K. Rabaey, R.A. Rozendal, Microbial electrosynthesis - revisiting the electrical route for microbial production, Nat. Rev. Microbiol. 8 (10) (2010) 706−716.

[6] L. Jourdin, T. Burdyny, Microbial electrosynthesis: where do we go from here? Trends Biotechnol. 39 (4) (2021) 359−369.

[7] J. Daniell, S. Nagaraju, F. Burton, M. Kopke, S.D. Simpson, Low-carbon fuel and chemical production by anaerobic gas fermentation, Advances in Biochemical

Engineering-Biotechnology 156 (2016) 293−321.

[8] G. Shang, K. Cui, W. Cai, X. Hu, P. Jin, K. Guo, A 20 L electrochemical continuous stirred-tank reactor for high rate microbial electrosynthesis of methane from CO_2, Chem. Eng. J. 451 (2023), 138898.

[9] M.C.A.A. Van Eerten-Jansen, A. Ter Heijne, T.I.M. Grootscholten, K.J.J. Steinbusch, T.H.J.A. Sleutels, H.V.M. Hamelers, C.J.N. Buisman, Bio-electrochemical production of caproate and caprylate from acetate by mixed cultures, ACS Sustain. Chem. Eng. 1 (5) (2013) 513−518.

[10] B. Bian, S. Bajracharya, J. Xu, D. Pant, P.E. Saikaly, Microbial electrosynthesis from CO_2: challenges, opportunities and perspectives in the context of circular bioeconomy, Bioresour. Technol. 302 (2020), 122863.

[11] R. Saini, R. Kapoor, R. Kumar, T.O. Siddiqi, A. Kumar, CO_2 utilizing microbes–a comprehensive review, Biotechnol. Adv. 29 (6) (2011) 949−960.

[12] S.W. Ragsdale, E. Pierce, Acetogenesis and the Wood-Ljungdahl pathway of CO_2 fixation, Biochim. Biophys. Acta 1784 (12) (2008) 1873−1898.

[13] H.L. Drake, A.S. Gossner, S.L. Daniel, Old acetogens, new light, Ann. N. Y. Acad. Sci. 1125 (2008) 100−128.

[14] J.S. Deutzmann, M. Sahin, A.M. Spormann, Extracellular enzymes facilitate electron uptake in biocorrosion and bioelectrosynthesis, mBio 6 (2) (2015) e00496-15.

[15] E.V. LaBelle, C.W. Marshall, H.D. May, Microbiome for the electrosynthesis of chemicals from carbon dioxide, Accounts Chem. Res. 53 (1) (2020) 62−71.

[16] O. Lefebvre, Z. Tan, S. Kharkwal, H.Y. Ng, Effect of increasing anodic NaCl concentration on microbial fuel cell performance, Bioresour. Technol. 112 (2012) 336−340.

[17] T.N. Zhilina, E.N. Detkova, F.A. Rainey, G.A. Osipov, A.M. Lysenko, N.A. Kostrikina, G.A. Zavarzin, *Natronoincola histidinovorans* gen. nov., sp. nov., a new alkaliphilic acetogenic anaerobe, Curr. Microbiol. 37 (3) (1998) 177−185.

[18] E.V. Pikuta, R.B. Hoover, A.K. Bej, D. Marsic, E.N. Detkova, W.B. Whitman, P. Krader, *Tindallia californiensis* sp nov., a new anaerobic, haloalkaliphilic, spore-forming acetogen isolated from Mono Lake in California, Extremophiles 7 (4) (2003) 327−334.

[19] M.F. Alqahtani, S. Bajracharya, K.P. Katuri, M. Ali, A.a. Ragab, G. Michoud, D. Daffonchio, P.E. Saikaly, Enrichment of marinobacter sp. and halophilic homoacetogens at the biocathode of microbial electrosynthesis system inoculated with red sea brine pool, Front. Microbiol. 10 (2019) 2563.

[20] M.F. Alqahtani, S. Bajracharya, K.P. Katuri, M. Ali, J. Xu, M.S. Alarawi, P.E. Saikaly, Enrichment of salt-tolerant CO_2-fixing communities in microbial electrosynthesis systems using porous ceramic hollow tube wrapped with carbon cloth as cathode and for CO2 supply, Sci. Total Environ. 766 (2021), 142668-142668.

[21] F.J. Millero, R. Feistel, D.G. Wright, T.J. McDougall, The composition of standard seawater and the definition of the reference-composition salinity scale, Deep-Sea Res. Part I Oceanogr. Res. Pap. 55 (1) (2008) 50−72.

[22] S.A. Patil, J.B.A. Arends, I. Vanwonterghem, J. van Meerbergen, K. Guo, G.W. Tyson, K. Rabaey, Selective enrichment establishes a stable performing community for microbial electrosynthesis of acetate from CO_2, Environ. Sci. Technol. 49 (14) (2015) 8833−8843.

[23] B. Bian, J. Xu, K.P. Katuri, P.E. Saikaly, Resistance assessment of microbial electrosynthesis for biochemical production to changes in delivery methods and CO_2 flow rates, Bioresour. Technol. (2021) 319.

[24] S. Bajracharya, K. Vanbroekhoven, C.J. Buisman, D. Pant, D.P. Strik, Application of gas diffusion biocathode in microbial electrosynthesis from carbon dioxide, Environ. Sci. Pollut. Res. Int. 23 (22) (2016) 22292−22308.

[25] F. Ameen, W.A. Alshehri, S.A. Nadhari, Effect of electroactive biofilm formation on acetic acid production in anaerobic sludge driven microbial electrosynthesis, ACS Sustain. Chem. Eng. 8 (1) (2019) 311−318.

[26] K. Guo, A. Prevoreau, K. Rabaey, A novel tubular microbial electrolysis cell for high rate hydrogen production, J. Power Sources 356 (2017) 484−490.

[27] M.A. Izquierdo-Gil, J.P.G. Villaluenga, S. Munoz, V.M. Barragan, The correlation between the water content and electrolyte permeability of cation-exchange membranes, Int. J. Mol. Sci. 21 (16) (2020) 5897.

[28] W. Li, Y. Nan, Q. You, Z. Jin, CO_2 solubility in brine in silica nanopores in relation to geological CO_2 sequestration in tight formations: effect of salinity and pH, Chem. Eng. J. 411 (2021), 127626.

[29] J.M. Pastor, M. Salvador, M. Argandona, V. Bernal, M. Reina-Bueno, L.N. Csonka, J.L. Iborra, C. Vargas, J.J. Nieto, M. Canovas, Ectoines in cell stress protection: uses and biotechnological production, Biotechnol. Adv. 28 (6) (2010) 782−801.

[30] F. Aulenta, L. Catapano, L. Snip, M. Villano, M. Majone, Linking bacterial metabolism to graphite cathodes: electrochemical insights into the H_2 -producing capability of *Desulfovibrio* sp, ChemSusChem 5 (6) (2012) 1080−1085.

[31] M. Roy, R. Yadav, P. Chiranjeevi, S.A. Patil, Direct utilization of industrial carbon dioxide with low impurities for acetate production via microbial electrosynthesis, Bioresour. Technol. 320 (2021), 124289.

[32] B.R. Dhar, J.-H. Park, H.-D. Park, H.-S. Lee, Hydrogen-based syntrophy in an electrically conductive biofilm anode, Chem. Eng. J. 359 (2019) 208−216.

[33] R. Mateos, A. Sotres, R.M. Alonso, A. Moran, A. Escapa, Enhanced CO_2 conversion to acetate through microbial electrosynthesis (MES) by continuous headspace gas recirculation, Energies 12 (17) (2019) 3297.

[34] K. Rabaey, N. Boon, M. Hofte, W. Verstraete, Microbial phenazine production enhances electron transfer in biofuel cells, Environ. Sci. Technol. 39 (9) (2005) 3401−3408.

[35] P.J. Carvalho, L.M.C. Pereira, N.P.F. Gonçalves, A.J. Queimada, J.A.P. Coutinho, Carbon dioxide solubility in aqueous solutions of NaCl: measurements and modeling with electrolyte equations of state, Fluid Phase Equil. 388 (2015) 100−106.

[36] G. Dubinina, M. Grabovich, N. Leshcheva, S. Gronow, E. Gavrish, V. Akimov, *Spirochaeta sinaica* sp. nov., a halophilic spirochaete isolated from a cyanobacterial mat, Int. J. Syst. Evol. Microbiol. 65 (11) (2015) 3872−3877.